Record low losses in TiO_2 channel waveguides

I. Hegeman, E. J. P. Vissers, M. Dijkstra, S.M. Martinussen, P. Muñoz Galindo and S. M. Garcia-Blanco

MESA+ Institute, University of Twente, P.O. Box 217, 7550 AE, Enschede, The Netherlands

TiO_2 is a promising material for waveguides, due to its wide transparency window of 370 nm to 5.9 um [1]*, high refractive index of 2.4 @ 1550 nm* [1]*, and a high nonlinear index of 2.3-3.6×10^{-18} m^2/W at 1550 nm* [2]*. We have fabricated TiO_2 channel waveguides on SiO_2 with record low propagation losses of 2.3±0.25 dB/cm at 1306 nm. These low losses have been achieved by optimizing the sputtering process to induce less crystallization, as well as optimizing the etching process for reduced sidewall roughness.*

Introduction

Research on TiO_2 as a waveguide material is rapidly growing since around 2010 [2–11]. Advantages of the use of TiO_2 for integrated photonic circuits are include the high refractive index around 2.4 [1,12], which allows to scale down the waveguide dimensions, the wide transparency window ranging from the visible till mid-IR wavelength range [1] and its large non-linear refractive index [3]. TiO_2 slab waveguides have been reported with slab losses as low as 0.4 dB/cm at 826 nm for amorphous layers [12] and 3.5 dB/cm at 826 nm for anatase polycrystalline layers [12]. The lowest losses in channel waveguides fabricated using reactive ion etching are 9.7 dB/cm at 632.8 nm [6] and 4 dB/cm at a 1550nm [7]. Losses as low as 7.5 dB/cm at 633 nm and 1.2 dB/cm at 1550 nm were obtained by using a dielectric lift-off fabrication process [9]. In contrary to the deposition shown in our work, all these layers were deposited using RF sputter deposition.

Applications of TiO_2 waveguides were shown using disk resonators fabricated using sol-gel TiO_2 layers [13]. Q-factors on the order of 10^5 were demonstrated. Also micro-bends and couplers were reported in TiO_2 [7], which allows the design of integrated optical devices. The high refractive index of TiO_2 permits the realization of highly efficient waveguides for waveguide-enhanced Raman spectroscopy [14]. The negative thermo-optic coefficient of -1×10^4 $°C^{-1}$ [11] makes TiO_2 a useful material to create athermal devices by combining TiO_2 with Si_3N_4 [11,15] or with silicon [8]. The high non-linear refractive index [1,2] together with the high linear refractive index makes TiO_2 a promising material for integrated non-linear devices. Octave spanning super continuum generation [3], third harmonic generation [10] and four-wave mixing [2] were demonstrated in TiO_2 waveguides.

Waveguide fabrication

Many applications have been demonstrated, however for TiO_2 to compete with other platforms such as Si_3N_4, the losses need to be decreased by optimizing the fabrication processes. We have fabricated TiO_2 channel waveguides by optimizing the deposition and etching process parameters.

In our work, the deposition of TiO_2 layers is performed by DC reactive sputtering, using a Ti target, a plasma consisting of 18% O_2 and 82% Ar, a process pressure of 6×10^{-3} mbar and 500 W DC power. The layers are deposited on top of a silicon wafer with a layer of 8 μm thick thermal SiO_2. No cladding is deposited on top of the waveguide.

Patterning of the TiO_2 layers is performed using UV-lithography followed by reactive ion etching. For the UV-lithography a layer of 1.7 µm thick photoresist is used. The reactive ion etching is done with the Oxford plasma pro 100 Cobra system. The etch parameters are summarized in table 1. Etch recipe A is the recipe as received from the producer of the system. Recipe B is as the recipe after optimization for etching TiO_2 waveguides. The ICP power is lowered in order to obtain a more homogeneous etching profile over the wafer. The process pressure is lowered in order to obtain sidewalls close to 90°.

Setting	**A**	**B**
SF_6	25 sccm	25 sccm
O_2	6 sccm	6 sccm
Ar	5 sccm	5 sccm
Pressure	40 mTorr	10 mTorr
ICP power	1850 W	1500 W
CCP power	20 W	20 W
Temperature	10 °C	10 °C

Table 1: RIE parameters for the etching process without optimization (A) and after optimization (B).

Characterization

SEM images of the resulting TiO_2 waveguides are shown in figure 1. The optimized etching recipe shows sidewalls with an average angle of 85.2°, making these waveguides suitable for all

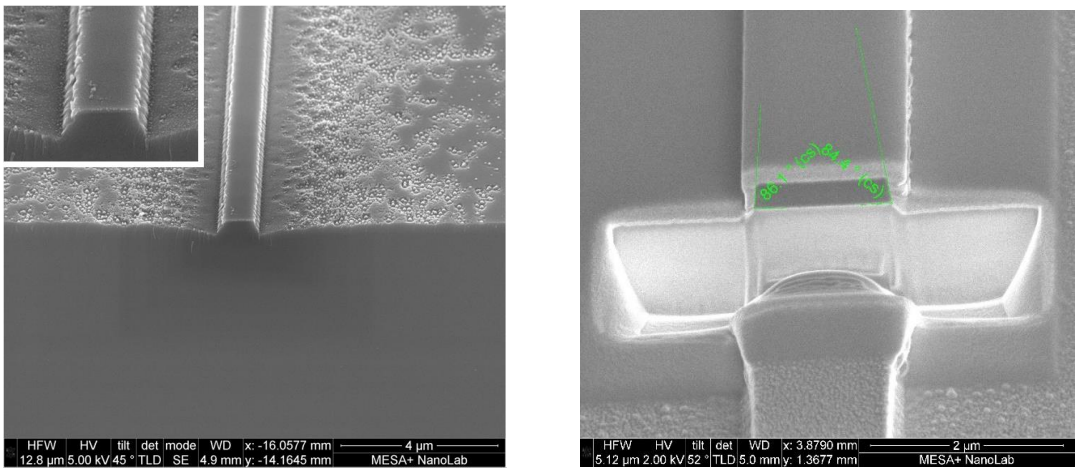

(a) (b)

Figure 1: TiO_2 waveguides with a thickness of 55 nm etched with recipe A (a) and with a thickness of 360 nm etched with recipe B (b).

kinds of structures including ring resonators with small bend radii and couplers. The sidewall roughness is also reduced by the more directional etching.

Figure 3b shows the Raman spectrum, showing a large peak at 520 cm^{-1} corresponding to the silicon wafer. The peaks at 385 cm^{-1} and 638 cm^{-1} indicate the presence of the anatase crystalline phase in the TiO_2 channel. Due to the nature of the sputter deposition the phase will be polycrystalline.

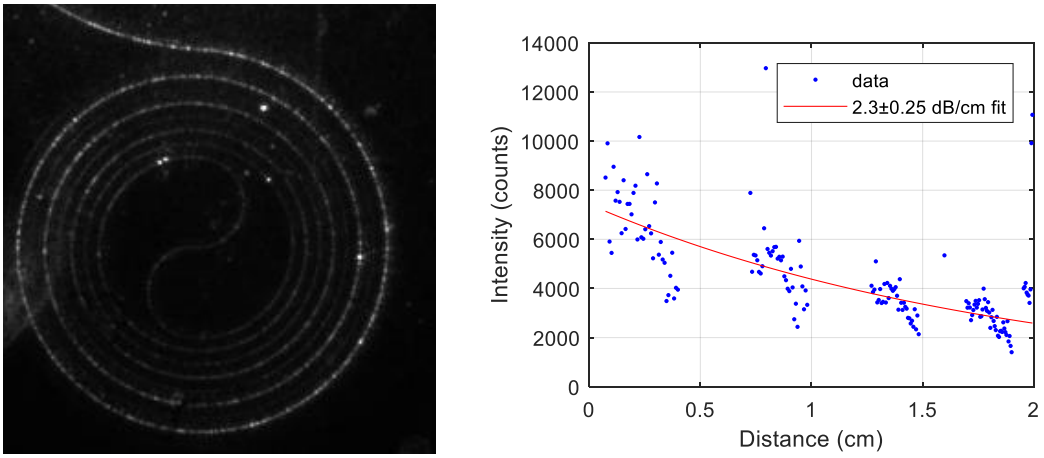

(a) (b)

Figure 2: (a) Photograph of the waveguide measured, with 1306 nm light coupled in; (b) Scattered light intensity vs propagated distance and a fit of the exponential decay.

The optical losses were characterized for a 360 nm thick TiO_2 waveguide etched using recipe B. The losses were measured at multiple wavelengths ranging from visible wavelengths to the mid-IR. Figure 2a shows a top view image of 1306 nm wavelength light coupled into a spiral waveguide. Figure 2b shows the scattered light intensity as a function of propagated distance. The optical losses are extracted from an exponential fit to the data. The resulting optical losses are 2.3±0.25 dB/cm which are, to our knowledge, the lowest losses at a wavelength of 1306 nm reported to date for etched TiO_2 channel waveguides.

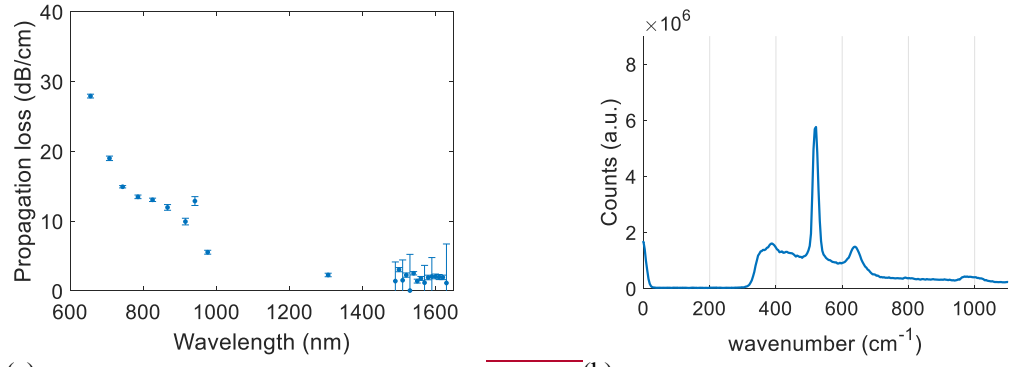

(a) (b)

Figure 3: (a) Optical losses as a for varying wavelengths; (b) Raman spectrum of the 360 nm thick TiO_2 waveguide, indicating the presence of the anatase crystalline phase.

Figure 3a shows the losses for varying wavelengths. For wavelengths between 1500 and 1650 nm the error bars increase significantly due to the high noise level compared to the small decay in intensity, so an accurate value for the losses was not obtained. For wavelengths below 1000 nm the losses increase significantly. One of the reasons is the increase of scattering losses with decreasing wavelength. Furthermore the waveguides support 2 TE modes around 1550 nm and at 1306 nm. Below 1000 nm the waveguide starts to support more modes, up to 8 TE modes at 632.8 nm, which makes the behavior of the waveguide unpredictable. The higher order modes could have higher losses compared to the fundamental mode.

Conclusion

In this work, we have shown polycrystalline anatase TiO_2 waveguides with losses as low as 2.3±0.25 dB/cm at a wavelength of 1306 nm, which is to our knowledge the lowest losses for reactive ion etched TiO_2 channel waveguides at this wavelength reported to date. The losses between 1500 and 1650 nm are close to the values obtained by Evans et. al. [7], where a lift-off process is used. The advantage of this fabrication process are the straight side walls, which allows to design micro ring resonators and optical couplers. In order to compare the losses at different wavelengths, the fabrication of single mode waveguides at varying wavelengths is necessary and it is currently ongoing.

Acknowledgements

NWO Industrial Doctorates 2018 program, under grant agreement NWA.ID.17.100 and European Research Council (ERC) Horizon 2020 research and innovation programme, grant agreement no. 648978 (RENOS).

1. J. Kischkat, S. Peters, B. Gruska, M. Semtsiv, M. Chashnikova, M. Klinkmüller, O. Fedosenko, S. Machulik, A. Aleksandrova, G. Monastyrskyi, Y. Flores, and W. Ted Masselink, "Mid-infrared optical properties of thin films of aluminum oxide, titanium dioxide, silicon dioxide, aluminum nitride, and silicon nitride," Appl. Opt. **51**, 6789 (2012).
2. X. Guan, H. Hu, L. K. Oxenløwe, and L. H. Frandsen, "Compact titanium dioxide waveguides with high nonlinearity at telecommunication wavelengths," Opt. Express **26**, 1055–1063 (2018).
3. K. Hammani, L. Markey, M. Lamy, B. Kibler, J. Arocas, J. Fatome, A. Dereux, J.-C. Weeber, and C. Finot, "Octave Spanning Supercontinuum in Titanium Dioxide Waveguides," Appl. Sci. **8**, 543 (2018).
4. M. Roussey, M. Häyrinen, a. Säynätjoki, V. Gandhi, L. Karvonen, P. Stenberg, M. Kuittinen, and S. Honkanen, "Low-loss titanium-dioxide strip waveguides by atomic layer deposition," SPIE Photonics West 2014-OPTO Optoelectron. Devices Mater. **8982**, 89820E (2014).
5. J. T. Choy, J. D. B. Bradley, P. B. Deotare, I. B. Burgess, C. C. Evans, E. Mazur, and M. Loncar, "Integrated TiO_2 resonators for visible photonics," **37**, 539–541 (2011).
6. M. Furuhashi, M. Fujiwara, T. Ohshiro, M. Tsutsui, K. Matsubara, M. Taniguchi, S. Takeuchi, and T. Kawai, "Development of microfabricated TiO_2 channel waveguides," AIP Adv. **1**, 032102 (2011).
7. J. D. B. Bradley, C. C. Evans, J. T. Choy, O. Reshef, B. Parag, F. Parsy, K. C. Phillips, M. Lon, and E. Mazur, "Submicrometer-wide amorphous and polycrystalline anatase TiO_2 waveguides for microphotonic devices," Opt. Express **20**, 8336–8346 (2012).
8. B. Guha, J. Cardenas, and M. Lipson, "Athermal silicon microring resonators with titanium oxide cladding," Opt. Express **21**, 26557 (2013).
9. C. C. Evans, C. Liu, and J. Suntivich, "Low-loss titanium dioxide waveguides and resonators using a dielectric lift-off fabrication process," Opt. Express **23**, 11160 (2015).
10. C. C. Evans, K. Shtyrkova, O. Reshef, M. Moebius, J. D. B. Bradley, S. Griesse-Nascimento, E. Ippen, and E. Mazur, "Multimode phase-matched third-harmonic generation in sub-micrometer-wide anatase TiO_2 waveguides," Opt. Express **23**, 7832–7841 (2015).
11. F. Qiu, A. M. Spring, and S. Yokoyama, "Athermal and high-Q hybrid TiO_2-Si_3N_4 ring resonator via an etching-free fabrication technique," ACS Photonics **2**, 405–409 (2015).
12. J. D. B. Bradley, C. C. Evans, F. Parsy, K. C. Phillips, R. Senaratne, E. Marti, and E. Mazur, "Low-loss TiO_2 planar waveguides for nanophotonic applications," in *2010 IEEE Photinic Society's 23rd Annual Meeting* (IEEE, 2010), pp. 313–314.
13. J. Park, S. K. Ozdemir, F. Monifi, T. Chadha, S. H. Huang, P. Biswas, and L. Yang, "Titanium Dioxide Whispering Gallery Microcavities," Adv. Opt. Mater. **2**, 711–717 (2014).
14. C. C. Evans, C. Liu, and J. Suntivich, "TiO_2 Nanophotonic Sensors for Efficient Integrated Evanescent Raman Spectroscopy," ACS Photonics **3**, 1662–1669 (2016).
15. L. He, Y. Guo, Z. Han, K. Wada, L. C. Kimerling, J. Michel, A. M. Agarwal, G. Li, and L. Zhang, "Broadband athermal waveguides and devices for datacom and telecom applications," Proc. SPIE - Int. Soc. Opt. Eng. **10537**, (2018).